Journal of Applied Analysis and Computation
Volume 17, Number 1, February 2027, 313–336
Website:http://www.jaac-online.com
DOI:10.11948/20250376

AN EFFICIENT ENERGY-PRESERVING SCHEME FOR NONLINEAR GENERALIZED DAMPED SPACE-FRACTIONAL KLEIN-GORDON EQUATION BASED ON THE MATRIX TRANSFER TECHNIQUE

Yuqing Lv[1], Yanming Zhang[2] and Yu Li[1,†]

Abstract This paper proposes a high-order and energy-preserving finite difference scheme for solving nonlinear generalized space-fractional damped Klein-Gordon equations. The scheme is conceptually straightforward and easy to implement. By employing the matrix transfer technique, a fully diagonal spatial discretization matrix is obtained, which significantly reduces computational and storage complexity. Combined with an extended Runge-Kutta-Nyström method in time, the fully discrete scheme achieves fourth-order accuracy in both space and time. The preservation of the dissipative or conservative of the energy for the nonlinear generalized space-fractional damped Klein-Gordon equations is rigorously proved across various physical settings. Numerical experiments confirm that the proposed scheme exhibits convergence to the exact solution and retains the physical properties of the original problem.

Keywords Nonlinear space fractional damped Klein-Gordon equation, fractional central difference scheme, matrix transfer technique, extended Runge-Kutta-Nyström method.

MSC(2010) 65L20, 26A33, 34A08.

1. Introduction

Recent astrophysical observations have renewed interest in the fractional Klein-Gordon equations (FKGE) as a fundamental model for spin-0 bosons and related quantum phenomena [1, 18, 19]. However, the FKGE presents profound mathematical and computational challenges due to the nonlocality of the fractional derivative operator. Thus, developing a high-order, energy-preserving numerical scheme for the FKGE is an important yet demanding task. Although several high-order methods exist [10, 13, 24], many are limited in practical applications due to dense discrete matrices or algorithmic complexity. To overcome these limitations, this paper introduces a novel finite difference scheme that combines high-order accuracy with a sparse, computationally efficient structure.

In this paper, we consider the following nonlinear generalized damped FKGE

$$u_{tt}(\boldsymbol{x},t)+J(t)(-\Delta)^{\alpha/2}u(\boldsymbol{x},t)+\kappa u_t(\boldsymbol{x},t)+G'(u(\boldsymbol{x},t))=0, \tag{1.1}$$

where $\boldsymbol{x}\in\Omega$, $t\in(0,T]$, and subject to initial conditions

$$u(\boldsymbol{x},0)=\varphi(\boldsymbol{x}),\quad u_t(\boldsymbol{x},0)=\mu(\boldsymbol{x}),\quad \boldsymbol{x}\in\Omega,$$

†The corresponding author.
[1]Department of Mathematics, Northeast Forestry University, Harbin 150040, China
[2]School of Mathematics and Computational Sciences, Hunan First Normal University, Changsha 410205, China
Email: 487810355@qq.com(Y. Lv), zhangyanming@outlook.com(Y. Zhang), liy@nefu.edu.cn(Y. Li)

where Ω is an open bounded domain. $G'(u)$ is assumed to be non-negative and smooth, and it represents the gradient of G, and $\kappa > 0$ denotes the non-negative damping. The Riesz space-fractional derivative $(-\Delta)^{\alpha/2}$, $1 < \alpha \leq 2$ is defined as [17]

$$-(-\Delta)^{\alpha/2}u = \frac{\partial^\alpha u}{\partial|x|^\alpha} = -c_\alpha \left({}_aD_x^\alpha u + {}_xD_b^\alpha u\right), \quad c_\alpha = \frac{1}{2\cos\frac{\pi\alpha}{2}},$$

where ${}_aD_x^\alpha$ and ${}_xD_b^\alpha$ for $x \in [a,b]$ are defined as

$${}_aD_x^\alpha f(x) = \frac{1}{\Gamma(n-\alpha)}\frac{\mathrm{d}^n}{\mathrm{d}x^n}\int_a^x \frac{f(t)}{(x-t)^{\alpha-n+1}}\mathrm{d}t,$$
$${}_xD_b^\alpha f(x) = \frac{(-1)^n}{\Gamma(n-\alpha)}\frac{\mathrm{d}^n}{\mathrm{d}x^n}\int_x^b \frac{f(t)}{(t-x)^{\alpha-n+1}}\mathrm{d}t.$$

The energy dissipation preserving property represents the most critical characteristic of system (1.1). As demonstrated in [23], the generalized energy function for this system can be expressed as

$$\mathcal{E}(t) = e^{\kappa t}\left[\frac{1}{2}\|u_t\|_{x,2}^2 + \frac{\kappa}{2}\langle u_t, u\rangle_x + \frac{J(t)}{2}\|(-\Delta)^{\alpha/4}u\|_{x,2}^2 + \langle G(u), 1\rangle_x\right], \tag{1.2}$$

which satisfies

$$\mathcal{E}'(t) = e^{\kappa t}\left[\frac{J'(t)}{2}\left\|(-\Delta)^{\alpha/4}u\right\|_{x,2}^2 - \frac{\kappa}{2}\langle G'(u), u\rangle_x + \kappa\langle G(u), 1\rangle_x\right], \quad t \in (0,T],$$

with the Hamiltonian energy density having the following form

$$\mathcal{H}(x,t) = e^{\kappa t}\left[\frac{1}{2}(u_t)^2 + \frac{\kappa}{2}u_t\cdot u + \frac{J(t)}{2}\left|(-\Delta)^{\alpha/4}u\right|^2 + G(u)\right],$$

where $1 = (1,1,\cdots,1)$, $\|\cdot\|_{x,p}$ represents the L^p norm in the spatial direction, $\langle\cdot,\cdot\rangle_x$ denotes the inner product defined by $\langle f, g\rangle = \int_a^b f(x)\overline{g(x)}\,dx$. The exponential factor $e^{\kappa t}$ can represent a scale factor, damping, or growth depending on the physical context. In the de Sitter spacetime considered in this work, it is related to the cosmological constant and describes the expansion of the universe.

In fact, the different choices of $J(t)$ in (1.1) have different practical significance in various domains. First, in cosmological contexts, $J(t)$ represents the scale factor characterizing universal expansion [14], while in other physical frameworks, $J(t)$ reduces to unity. Second, the functional forms of $J(t)$ and potential $G(u)$ collectively determine both the equation's physical interpretation and corresponding energy evolution. For instance, when modeling nonlinear superradiant phenomena in condensed matter systems [3], this equation yields a context-specific energy functional as demonstrated in the following examples. Specific examples below illustrate these physical frameworks and corresponding energy functionals.

Example 1.1. The system (1.1) can describe the nonlinear supratransmission phenomenon by determining the coefficient as $\alpha = 2$ and $J(t) = 1$, $G(u) = \frac{1}{2!}u^2 - \frac{1}{4!}u^4 + \frac{1}{6!}u^6$ with $\kappa = 0$, which has the energy formula [3]

$$\mathcal{E}(t) = \frac{1}{2}\|u_t\|_{x,2}^2 + \frac{1}{2}\left\|(-\Delta)u\right\|_{x,2}^2 + \frac{1}{2!}\|u\|_{x,2}^2 - \frac{1}{4!}\|u\|_{x,4}^4 + \frac{1}{6!}\|u\|_{x,6}^6,$$

where the related Hamiltonian density has the form

$$\mathcal{H}(x,t)=\frac{1}{2}u_t^2+\frac{1}{2}\left[(-\Delta)u\right]^2+\frac{1}{2!}u^2-\frac{1}{4!}u^4+\frac{1}{6!}u^6.$$

In nonlinear regimes, the nonlinear supratransmission is a special phenomenon observed in nonlinear media. Specifically, when one end of a semi-infinite nonlinear chain is subjected to a harmonic perturbation, if the perturbation frequency falls within the forbidden band gap, the amplitude of the wave signals in the chain will suddenly increase. This phenomenon has been observed in both classical and fractional Klein-Gordon systems and is of great significance for understanding energy transfer and signal propagation in nonlinear media. Furthermore, the energy of the damped FKGE in nonlinear supratransmission is conserved.

Example 1.2. In Cosmology, the Einstein equation is a significant theory for studying dark energy and cosmic acceleration [25], and the de Sitter spacetime, composed of exact solutions to the Einstein equation, provides a mathematical model to describe the fundamental geometry of the Universe. Furthermore, in the context of quantum field theory, the quantum fields described by the Klein-Gordon equation evolve in curved spacetime, the geometry of which is constituted by de Sitter spacetime. In [23], Takuya and Makoto specifically discussed the varying properties and phenomena of FKGE with the change of the Hubble constant. We can rewrite the system (1.1) by setting $\kappa=nH$, $J(t)=c^2e^{-2Ht}$ with the scalar potential $G(u)=\frac{m^2c^4}{2\hbar^2}u^2+\frac{\lambda c^2}{q+1}|u|^{q+1}$. In this case, it has the following energy formula

$$\mathcal{E}(t)=\frac{1}{c}e^{nHt}\left[\frac{1}{2}\|u_t\|^2+\frac{nH}{2}\langle u_t,u\rangle_x+\frac{1}{2}c^2e^{-2Ht}\|(-\Delta)^{\alpha/4}u\|^2+\frac{m^2c^4}{2\hbar^2}\|u\|^2+\frac{\lambda c^2}{q+1}\|u\|^{q+1}\right],$$

and the related Hamiltonian density is

$$\mathcal{H}(t)=\frac{1}{2c}e^{nHt}\left[u_t^2+nHu_t\cdot u+c^2e^{-2Ht}\left[(-\Delta)^{\alpha/4}u\right]^2+\frac{m^2c^4}{\hbar^2}u^2+\frac{2\lambda c^2}{q+1}u^{q+1}\right],$$

where $n\geq 1$ represents the spatial dimension and $c>0$ is the speed of light.

When $H>0$, the space expands and the energy is dissipated, leading to property $E(t)<E(0)$. On the other hand, when $H<0$, the space is contracting and the equation is anti-dissipative, resulting in $E(t)>E(0)$. Particularly, in quantum field theory, investigating the Higgs boson's role is significant for elucidating the fundamental enigmas of the universe and understanding the mass of elementary particles. We can explore the Higgs boson system by choosing $J(t)=e^{-2t}$, $\kappa=n$ and letting $G(u)=\frac{1}{2}\gamma^2u^2+\frac{\lambda}{m+1}|u|^{m+1}$. For the case $n=1$, the total energy of the Higgs boson system is

$$\mathcal{E}(t)=e^t\left[\frac{1}{2}\left\|u_t+\frac{1}{2}u\right\|^2+\frac{e^{-2t}}{2}\left\|(-\Delta)^{\alpha/4}u\right\|_{x,2}^2-\frac{1}{2}\left(\frac{1}{4}+\gamma^2\right)\|u\|_{x,2}^2+\frac{\lambda}{m+1}\|u\|_{x,m+1}^{m+1}\right],$$

with

$$\mathcal{E}'(t)=-e^t\left[e^{-2t}\left\|(-\Delta)^{\alpha/4}u\right\|_{x,2}^2+\frac{\lambda(m-1)}{2(m+1)}\|u\|_{x,m+1}^{m+1}\right].$$

As shown in [4], the energy of the Higgs boson system is dissipative. In summary, we have observed that the energy formulation of a system varies depending on the specific physical context, and the aforementioned generalized energy formulation (1.2) is able to successfully explore the energy conservation of the FKGE in various fields.

Despite its broad applicability, the FKGE's computational complexity poses significant challenges, necessitating the development of robust numerical methods for accurate and efficient solutions. In recent years, significant progress has been made in the development of numerical methods for various types of fractional wave equations that strictly preserve structures [9, 11, 22, 27]. In [9], a new fourth-order average vector field finite difference method in time and fourth-order weighted and shifted Lubich difference operator in space were used to develop a fourth-order energy-preserving scheme for nonlinear space-fractional wave equations. Zhou et al. [27] developed a fourth-order central difference scheme for spatial discretization and the semi-implicit Crank-Nicolson scheme for temporal discretization. Sun et al. [22] efficiently constructed numerical solutions via the adoption of a shifted convolution quadrature formula for approximating the two-dimensional spatial fractional derivative. Jiang and Hu [11] introduced a new class of linearly implicit, dissipation-preserving spectral schemes for solving space-fractional nonlinear wave equations. The proposed spectral method achieves a transition from algebraic convergence $O(h^4)$ to exponential convergence $O(e^{-cN})$. However, for the nonlinear space fractional damped Klein-Gordon equation, which has an important physical background, there has been relatively little development of numerical methods that can simultaneously satisfy the requirements of high accuracy and stringent structure preservation. Tsuchiya and Nakamura [23] achieved the high-performance computation of the integer-order case of the equation but did not address the fractional case. Subsequently, Hendy et al. [8] developed the numerical study of this equation to fractional order by constructing a format that preserves the energy dissipation law via the Legendre-Galerkin spectral method which achieved high accuracy in spatial discretization. However, the development of high-order, easy-to-code numerical methods which can be effectively extended to two-dimensional problems remains a valuable objective.

In this paper, we propose a novel numerical scheme for the nonlinear generalized damped FKGE that is both easily programmable and exhibits fourth-order accuracy. For spatial discretization of the FKGE problem (1.1), we present a fourth-order central difference scheme based on the matrix transfer technique (MTT), which can produce a full diagonal matrix expression of the approximation of the Riesz fractional derivative. Based on the matrix properties, we prove the energy-preserving property for the proposed semi-discrete scheme. Then, a fourth-order extended Runge-Kutta-Nyström (ERKN) method is used to process temporal discretization. A further benefit of the proposed method is extending the application to two or higher spatial dimensions. The convergence, effectiveness, and accuracy of the numerical method are verified by the numerical experiments.

The outline of this paper is as follows. In Section 2, we introduce a numerical method to solve the one-dimensional nonlinear generalized damped FKGE, and give some relevant lemmas, theorems of the energy dissipation-preserving property for the semi-discrete system. Then, the numerical method is extended to the multi-dimensional problems. In Section 3, various numerical experiments are presented to demonstrate the accuracy and convergence of the proposed method.

2. An efficient energy-preserving scheme and its properties

In this section, we present a fourth-order fully discrete scheme of the nonlinear generalized damped FKGE (1.1) under the different boundary conditions. We also discuss the various properties of the numerical method.

2.1. Spatial discretization

Considering the system (1.1) in the open bounded domain $\Omega = \{x_a < x < x_b\}$. We have the uniform space grid points $\boldsymbol{x} = \{x_0, x_1, \ldots, x_N\}$ with $x_0 = x_a$, $x_i = x_0 + i \times h$, and $h = (x_b - x_a)/N$. Assume $u_i = u(x_i, t)$, $i = 0 \ldots N$, is the numerical solution of (1.1). In this part, to simplify the computation of the spatial discretization of the nonlinear generalized damped FKGE, we propose the MTT based on the fourth-order central difference method. The main idea is to approximate the Riesz space-fractional derivative $(-\Delta)^{\alpha/2}$ by introducing a matrix representation $L^{\alpha/2}$. Therefore, we give the introduction of MTT corresponding to different boundary conditions [5].

2.1.1. Matrix transfer technique for the Dirichlet boundary condition

For the homogeneous Dirichlet boundary condition

$$u(x,t) = 0, \quad (x,t) \in \partial\Omega \times (0,T], \tag{2.1}$$

we suppose $\mathbf{u} = (u_1, u_2, \ldots, u_{N-1})^T$, and the following lemma will be used to derive the semi-discrete formulation of the nonlinear generalized damped FKGE.

Lemma 2.1. [21] *For the general tridiagonal Toeplitz matrix*

$$D = \begin{bmatrix} b & a & 0 & 0 & \cdots & 0 \\ c & b & a & 0 & \cdots & 0 \\ 0 & c & b & a & \cdots & 0 \\ \vdots & \vdots & \vdots & \vdots & \ddots & \vdots \\ 0 & \cdots & c & b & a & 0 \\ 0 & \cdots & 0 & c & b & a \\ 0 & \cdots & 0 & 0 & c & b \end{bmatrix}_{(N-1)\times(N-1)},$$

of order $N-1$, the eigenvectors and eigenvalues of the matrix D are described by

$$\lambda_i = b + 2a\sqrt{\frac{c}{a}}\cos\left(\frac{i\pi}{N}\right),$$

and

$$\xi_i = \left(\left(\frac{c}{a}\right)^{\frac{1}{2}}\sin\left(\frac{i\pi}{N}\right), \left(\frac{c}{a}\right)^{\frac{2}{2}}\sin\left(\frac{2i\pi}{N}\right), \cdots, \left(\frac{c}{a}\right)^{\frac{N-1}{2}}\sin\left(\frac{(N-1)i\pi}{N}\right)\right)^{\mathrm{T}},$$

for $i = 1, 2, \ldots, N-1$. Furthermore, the matrix D can be diagonalized by the matrix $P = (\xi_1, \xi_2, \ldots, \xi_{N-1})$, which reads as $P^{-1}DP = \Lambda$, where Λ is a diagonal matrix containing the eigenvalues of D, that is $\Lambda = diag(\lambda_1, \lambda_2, \ldots, \lambda_{N-1})$.

The proof of Lemma 2.1 and other details can be referred to [21].

Next, for the vector $\mathbf{u} = (u_1, u_2, \ldots, u_{N-1})^T$, we define the discrete second-order central difference operator δ_x^2 as

$$\delta_x^2 u_i = u_{i-1} - 2u_i + u_{i+1}, \tag{2.2}$$

for $i = 1, 2, \ldots, N-1$. Under the boundary condition (2.1), the matrix representation of the second-order operator (2.2) can be expressed as

$$M = \begin{bmatrix} -2 & 1 & & & & \\ 1 & -2 & 1 & & & \\ & \ddots & \ddots & \ddots & & \\ & & 1 & -2 & 1 & \\ & & & 1 & -2 & 1 \\ & & & & 1 & -2 \end{bmatrix}. \tag{2.3}$$

According to [5], we use the compact fourth-order difference operator $(-\Delta)_h$ for approximating the standard Laplacian $-\Delta$ as $(-\Delta)_h u(x) = (-\Delta)u(x) + \mathcal{O}(h^4)$, where

$$(-\Delta)_h = -\frac{1}{h^2}(1 + \frac{1}{12}\delta_x^2)^{-1}\delta_x^2. \tag{2.4}$$

Therefore, applying the compact difference scheme (2.4) to the grid function, we denote $L = A^{-1}B$ as the matrix representation of the differential operator $(-\Delta)_h$. The tridiagonal matrices A and B are given by

$$B = -\frac{1}{h^2}M, \quad A = (I + \frac{1}{12}M), \tag{2.5}$$

where the matrix M is defined in (2.3). Then $L\mathbf{u}$ approximates $(-\Delta)_h\mathbf{u}$ on the discrete grid.

Since the matrices A and B are tridiagonal Toeplitz matrices, according to Lemma 2.1, we find that matrices A and B can be diagonalized by matrices $P_A = \left(\xi_1^A, \xi_2^A, \cdots, \xi_{N-1}^A\right)$ and $P_B = \left(\xi_1^B, \xi_2^B, \cdots, \xi_{N-1}^B\right)$, such that $A = P_A \Lambda_A P_A^{-1}$ and $B = P_B \Lambda_B P_B^{-1}$, where $\Lambda_A = \operatorname{diag}\left(\lambda_1^A, \lambda_2^A, \cdots, \lambda_{N-1}^A\right)$ and $\Lambda_B = \operatorname{diag}\left(\lambda_1^B, \lambda_2^B, \cdots, \lambda_{N-1}^B\right)$. Here, λ_i^A, λ_i^B and ξ_i^A, ξ_i^B for $i = 1, 2, \ldots, N-1$ are eigenvalues and eigenvectors of A and B, respectively. Thus, the matrix L can be diagonalized as

$$L = (A^{-1}B) = (P_A \Lambda_A P_A^{-1})^{-1} P_B \Lambda_B P_B^{-1} = P \Lambda_A^{-1} \Lambda_B P^{-1}.$$

Based on Lemma 2.1 and the fact that both P_A and P_B are symmetric matrices, we conclude that $P_A = P_B$. To conveniently represent matrices, we denote $P = P_A = P_B$ and

$$\Lambda = \Lambda_A^{-1}\Lambda_B = \operatorname{diag}\left(\frac{\lambda_1^B}{\lambda_1^A}, \frac{\lambda_2^B}{\lambda_2^A}, \cdots, \frac{\lambda_{N-1}^B}{\lambda_{N-1}^A}\right).$$

In the preceding part, we introduced the MTT for the integer derivatives. In the subsequent discussion, we propose the MTT for the Riesz space-fractional derivative based on the preceding method.

Lemma 2.2. [28] *Assume the matrix D is positive definite and $D = P\Lambda P^{-1}$. Subsequently, for arbitrary real α, we have $D^\alpha = P\Lambda^\alpha P^{-1}$, which is uniquely determined by D and α.*

Since the matrices A and B are symmetric positive definite, according to Lemma 2.1 and 2.2, we obtain the following matrix representation of the discrete fractional operator $(-\Delta)_h^{\alpha/2}$ as

$$L^{\alpha/2} = P\Lambda^{\alpha/2}P^{-1}, \tag{2.6}$$

where

$$\Lambda = \operatorname{diag}(\lambda_1, \lambda_2, \cdots, \lambda_{N-1}), \quad \lambda_n = \frac{4\sin^2(\frac{n\pi}{2N})}{h^2(1-\frac{1}{3}\sin^2(\frac{n\pi}{2N}))}, \quad 1 \leqslant n \leqslant N-1,$$

and

$$P_{i,j} = \sin\left(\frac{ij\pi}{N}\right), \quad i,j = 1,\ldots,N-1. \tag{2.7}$$

Substituting (2.6) into (1.1) constructs the spatial discretization of the nonlinear generalized damped FKGE as

$$\mathbf{u}_{tt} + J(t)P\Lambda^{\alpha/2}P^{-1}\mathbf{u} + \kappa\mathbf{u}_t + G'(\mathbf{u}) = 0. \tag{2.8}$$

By multiplying P^{-1} on both sides of the equation (2.8), and supposing $\tilde{\mathbf{u}} = P^{-1}\mathbf{u}$, $\widetilde{G'(\mathbf{u})} = P^{-1}G'(\mathbf{u})$, $\tilde{\mathbf{u}}_{tt} = P^{-1}\mathbf{u}_{tt}$ and $\tilde{\mathbf{u}}_t = P^{-1}\mathbf{u}_t$, we finally obtain the spatial discretization of one-dimensional nonlinear generalized damped FKGE with Dirichlet boundary condition as

$$\tilde{\mathbf{u}}_{tt} + J(t)\Lambda^{\alpha/2}\tilde{\mathbf{u}} + \kappa\tilde{\mathbf{u}}_t + \widetilde{G'(\mathbf{u})} = 0, \tag{2.9}$$

where $\widetilde{G'(\mathbf{u})} = (\widetilde{G'(u_1,t)},\ldots,\widetilde{G'(u_N,t)})$. According to [16] and the definition of P^{-1} in (2.7), the matrix P^{-1} has a special structure such that applying it to a vector $\mathbf{u}$ is equivalent to performing the inverse discrete sine transform on $\mathbf{u}$. Similarly, $P\mathbf{u}$ corresponds to the discrete sine transform. Therefore, in our implementation, we replace $P^{-1}\mathbf{u}$ with inverse discrete sine transform and $P\mathbf{u}$ with discrete sine transform. Both transforms are computed efficiently using FFT-based algorithms.

As we know that the matrix expression of the Riesz space-fractional derivative is influenced by the different boundaries, we are going to imitate the preceding section to give the MTT for the Neumann boundary condition.

2.1.2. Matrix transfer technique for the Neumann boundary condition

For the Neumann boundary condition

$$u_x(x,t) = 0, \quad (x,t) \in \partial\Omega \times (0,T],$$

the corresponding matrices $A_{N+1\times N+1}$, $B_{N+1\times N+1}$ can be express as

$$A = \begin{bmatrix} \frac{5}{6} & \frac{1}{6} & 0 & \cdots & 0 & 0 \\ \frac{1}{12} & \frac{5}{6} & \frac{1}{12} & 0 & \cdots & 0 \\ 0 & \frac{1}{12} & \frac{5}{6} & \frac{1}{12} & 0 & \cdots \\ \vdots & \ddots & \ddots & \ddots & & \vdots \\ 0 & \cdots & \frac{1}{12} & \frac{5}{6} & \frac{1}{12} & 0 \\ 0 & \cdots & 0 & \frac{1}{12} & \frac{5}{6} & \frac{1}{12} \\ 0 & \cdots & 0 & 0 & \frac{1}{6} & \frac{5}{6} \end{bmatrix}, \quad B = h^{-2}\begin{bmatrix} 2 & -2 & 0 & \cdots & 0 & 0 \\ -1 & 2 & -1 & 0 & \cdots & 0 \\ 0 & -1 & 2 & -1 & 0 & \cdots \\ \vdots & \ddots & \ddots & \ddots & & \vdots \\ \cdots & 0 & -1 & 2 & -1 & 0 \\ 0 & \cdots & 0 & -1 & 2 & -1 \\ 0 & 0 & \cdots & 0 & -2 & 2 \end{bmatrix}.$$

Then, based on Section 2.1.1, the matrices Λ and P in the matrix representation of the Riesz space-fractional derivative (2.6) with homogeneous Neumann boundary condition are

$$\Lambda = \mathrm{diag}(\lambda_0, \lambda_2, \cdots, \lambda_N), \quad \lambda_n = \frac{4\sin^2(\frac{n\pi}{2N})}{h^2(1-\frac{1}{3}\sin^2(\frac{n\pi}{2N}))}, \quad 0 \leqslant n \leqslant N,$$

and

$$P_{i,j} = \cos\left(\frac{ij\pi}{N}\right), \quad i,j = 0,\ldots,N. \tag{2.10}$$

Analogously, we obtain that the spatial discretization of one-dimensional FKGE with homogeneous Neumann boundary conditions which is similar to scheme (2.9). And, we use the FFT-based fast algorithm [12] to reduce the computation complexity of the $P\mathbf{u}$ or $P^{-1}\mathbf{u}$.

2.2. Properties of the semi-discrete system

In this section, we introduce the fractional Sobolev norm and the relevant lemmas to study the energy property of the semi-discrete system of the general damped FKGE. First of all, we consider $h\mathbb{Z} = \{x_i = ih, i = 1\ldots N\}$ to be the infinite grid. For any grid functions $\mathbf{u} = \{u_i = u(x_i,t)\}$, $\mathbf{v} = \{v_i = v(x_i,t)\}$ defined on $h\mathbb{Z}$, we denote the discrete inner product and the associated L_h norm by

$$\langle \mathbf{u}, \mathbf{v}\rangle_h = h\sum_{i=1}^{N} u_i\bar{v}_i, \quad \|\mathbf{u}\|_{L_h^2} = \sqrt{\langle \mathbf{u}, \mathbf{u}\rangle_h},$$

where $\bar{v}$ is the complex conjugate of v, denote $L_h^2 = \{\mathbf{u}|\mathbf{u} = \{u_i\}, \|\mathbf{u}\|_{L_h} < \infty\}$. The fractional Sobolev space is the closure of $C^\infty(\Omega)$ is defined as

$$H^\psi(\Omega) = \left\{\mathbf{u} \in L^2(\Omega) \,\middle|\, |\omega|^\psi \mathcal{F}(\hat{\mathbf{u}}) \in L^2(\mathbb{R})\right\}.$$

Lemma 2.3 (Adjoint property)**.** *Let* $1 < \psi < 2$, $\mathbf{u} \in H_0^\psi(\Omega)$, $\mathbf{v} \in H_0^{\frac{\psi}{2}}(\Omega)$, *it holds*

$$\left\langle {}_aD_x^\psi \mathbf{u}, \mathbf{v}\right\rangle_{0,\Omega} = \left\langle {}_aD_x^{\psi/2}\mathbf{u}, {}_xD_b^{\psi/2}\mathbf{v}\right\rangle_{0,\Omega}, \quad \left\langle {}_xD_b^\psi \mathbf{u}, \mathbf{v}\right\rangle_{0,\Omega} = \left\langle {}_xD_b^{\psi/2}\mathbf{u}, {}_aD_x^{\psi/2}\mathbf{v}\right\rangle_{0,\Omega}.$$

Then, we have the semi-norm and the norm

$$|\mathbf{u}|_{\alpha/2} = \sqrt{\mathcal{D}\langle \mathbf{u}, \mathbf{u}\rangle_{0,\Omega}}, \quad \|\mathbf{u}\|_{\alpha/2} = \left(\|\mathbf{u}\|^2 + |\mathbf{u}|_{\alpha/2}^2\right)^{\frac{1}{2}},$$

where

$$\mathcal{D}\langle \mathbf{u}, \mathbf{v}\rangle_{0,\Omega} := -\left\langle \frac{\partial^\alpha \mathbf{u}}{\partial|x|^\alpha}, \mathbf{v}\right\rangle_{0,\Omega} = c_\alpha\left[\left\langle {}_aD_x^{\alpha/2}\mathbf{u}, {}_xD_b^{\alpha/2}\mathbf{v}\right\rangle_{0,\Omega} + \left\langle {}_xD_b^{\alpha/2}\mathbf{u}, {}_aD_x^{\alpha/2}\mathbf{v}\right\rangle_{0,\Omega}\right].$$

Lemma 2.4. *For any two grid functions* $\mathbf{u}^n$, $\mathbf{v}^n$, *there exists a unique square root operator* $\Lambda^{\alpha/4}$ *of the symmetric positive definite matrix* $\Lambda^{\alpha/2}$ *such that*

$$\langle \Lambda^{\alpha/2}\mathbf{u}^n, \mathbf{v}^n\rangle = \langle \Lambda^{\alpha/4}\mathbf{u}^n, \Lambda^{\alpha/4}\mathbf{v}^n\rangle.$$

Theorem 2.1 (Structure preserving property of the semi-discrete system)**.** *Owing to the solution of semi-discrete system* (2.8)*, we have the following identity*

$$\frac{d}{dt}\mathcal{E}_N(t) = e^{\kappa t}[\frac{1}{2}J'(t)\langle\Lambda^{\alpha/2}\tilde{\mathbf{u}},\tilde{\mathbf{u}}\rangle - \frac{\kappa}{2}\langle\widetilde{G'(\mathbf{u})},\tilde{\mathbf{u}}\rangle + \kappa\langle\widetilde{G(\mathbf{u})},1\rangle],$$

where

$$\mathcal{E}_N(t) = e^{\kappa t}\left[\frac{1}{2}\|\tilde{\mathbf{u}}_t\|^2 + \frac{J(t)}{2}|\tilde{\mathbf{u}}|^2_{\alpha/2} + \frac{\kappa}{2}\langle\tilde{\mathbf{u}}_t,\tilde{\mathbf{u}}\rangle + \langle\widetilde{G(\mathbf{u})},1\rangle\right]. \tag{2.11}$$

Proof. For the semi-discrete energy scheme (2.11), the following identities hold

$$\frac{d}{dt}\left[\frac{e^{\kappa t}}{2}\|\tilde{\mathbf{u}}_t\|^2\right] = \kappa\frac{e^{\kappa t}}{2}\|\tilde{\mathbf{u}}_t\|^2 + \frac{e^{\kappa t}}{2}\frac{d}{dt}\|\tilde{\mathbf{u}}_t\|^2 = \frac{1}{2}\kappa e^{\kappa t}\|\tilde{\mathbf{u}}_t\|^2 + e^{\kappa t}\langle\tilde{\mathbf{u}}_{tt},\tilde{\mathbf{u}}_t\rangle, \tag{2.12}$$

$$\begin{aligned}\frac{d}{dt}\left[\frac{\kappa e^{\kappa t}}{2}\langle\tilde{\mathbf{u}}_t,\tilde{\mathbf{u}}\rangle\right] &= \frac{\kappa^2}{2}e^{\kappa t}\langle\tilde{\mathbf{u}}_t,\tilde{\mathbf{u}}\rangle + \frac{\kappa}{2}e^{\kappa t}\frac{d}{dt}\langle\tilde{\mathbf{u}}_t,\tilde{\mathbf{u}}\rangle \\ &= \frac{\kappa^2}{2}e^{\kappa t}\langle\tilde{\mathbf{u}}_t,\tilde{\mathbf{u}}\rangle + \frac{\kappa}{2}e^{\kappa t}\langle\tilde{\mathbf{u}}_{tt},\tilde{\mathbf{u}}\rangle + \frac{\kappa}{2}e^{\kappa t}\langle\tilde{\mathbf{u}}_t,\tilde{\mathbf{u}}_t\rangle,\end{aligned} \tag{2.13}$$

$$\begin{aligned}\frac{d}{dt}\left[\frac{e^{\kappa t}J(t)}{2}|\tilde{\mathbf{u}}|^2_{\alpha/2}\right] &= \frac{\kappa}{2}e^{\kappa t}J(t)|\tilde{\mathbf{u}}|^2_{\alpha/2} + \frac{1}{2}e^{\kappa t}J'(t)|\tilde{\mathbf{u}}|^2_{\alpha/2} + \frac{1}{2}e^{\kappa t}J(t)\frac{d}{dt}|\tilde{\mathbf{u}}|^2_{\alpha/2} \\ &= \frac{\kappa}{2}e^{\kappa t}J(t)\langle\Lambda^{\alpha/2}\tilde{\mathbf{u}},\tilde{\mathbf{u}}\rangle + \frac{1}{2}e^{\kappa t}J'(t)\langle\Lambda^{\alpha/2}\tilde{\mathbf{u}},\tilde{\mathbf{u}}\rangle + e^{\kappa t}J(t)\langle\Lambda^{\alpha/2}\tilde{\mathbf{u}},\tilde{\mathbf{u}}_t\rangle,\end{aligned} \tag{2.14}$$

$$\frac{d}{dt}\left[e^{\kappa t}\langle\widetilde{G(\mathbf{u})},1\rangle\right] = \kappa e^{\kappa t}\langle\widetilde{G(\mathbf{u})},1\rangle + e^{\kappa t}\frac{d}{dt}\langle\widetilde{G(\mathbf{u})},1\rangle = \kappa e^{\kappa t}\langle\widetilde{G(\mathbf{u})},1\rangle + e^{\kappa t}\langle\widetilde{G'(\mathbf{u})},\tilde{\mathbf{u}}_t\rangle. \tag{2.15}$$

Performing the discrete inner product of equation (2.8) with u_t and multiplying equation (1.1) by $e^{\kappa t}$, we obtain

$$e^{\kappa t}\langle\tilde{\mathbf{u}}_{tt},\tilde{\mathbf{u}}_t\rangle = -e^{\kappa t}\kappa\langle\tilde{\mathbf{u}}_t,\tilde{\mathbf{u}}_t\rangle - e^{\kappa t}J(t)\langle\Lambda^{\alpha/2}\tilde{\mathbf{u}},\tilde{\mathbf{u}}_t\rangle - e^{\kappa t}\langle\widetilde{G'(\mathbf{u})},\tilde{\mathbf{u}}_t\rangle. \tag{2.16}$$

Multiplying the both sides of equation (2.8) by $\frac{\kappa}{2}e^{\kappa t}$ and computing the discrete inner product of (2.8) with u, the result reads as following

$$\frac{\kappa}{2}e^{\kappa t}\langle\tilde{\mathbf{u}}_{tt},\tilde{\mathbf{u}}\rangle = -\frac{\kappa^2}{2}e^{\kappa t}\langle\tilde{\mathbf{u}}_t,\tilde{\mathbf{u}}\rangle - \frac{\kappa}{2}e^{\kappa t}J(t)\langle\Lambda^{\alpha/2}\tilde{\mathbf{u}},\tilde{\mathbf{u}}\rangle - \frac{\kappa}{2}e^{\kappa t}\langle\widetilde{G'(\mathbf{u})},\tilde{\mathbf{u}}\rangle. \tag{2.17}$$

Substituting (2.12)-(2.17) into (2.11), the consequence can be quickly demonstrated. □

Theorem 2.1 establishes the energy-time relationship for the semi-discrete system. To better understand this property, we present two further examples.

In Example 1.1, when $J(t)$ and $G(u)$ are specified that $J(t) = c^2e^{-2Ht}$ and $G(\tilde{\mathbf{u}}) = \frac{m^2c^4}{2\hbar^2}u^2 + \frac{\lambda c^2}{q+1}|u|^{q+1}$, then we have $J'(t) = -2Hc^2e^{-2Ht}$ and $G'(\tilde{\mathbf{u}}) = \frac{m^2c^4}{\hbar^2}\tilde{\mathbf{u}} + \lambda c^2|\tilde{\mathbf{u}}|^{q-1}\tilde{\mathbf{u}}$, so the energy of Example 1.1 is given by

$$\mathcal{E}_N(t) = \frac{1}{c}e^{nHt}[\frac{1}{2}\|\tilde{\mathbf{u}}_t\|^2 + \frac{nH}{2}\langle\tilde{\mathbf{u}}_t,\tilde{\mathbf{u}}\rangle + \frac{1}{2}c^2e^{-2Ht}\|\Lambda^{\alpha/4}\tilde{\mathbf{u}}\|^2 + \frac{m^2c^4}{2\hbar^2}\|\tilde{\mathbf{u}}\|^2 + \frac{\lambda c^2}{q+1}\|\tilde{\mathbf{u}}\|^{q+1}].$$

According to the Theorem 2.1, we contain

$$\frac{d}{dt}\mathcal{E}_N(t) = \frac{1}{c}e^{nHt}[-Hc^2e^{-2Ht}\|\Lambda^{\alpha/4}\tilde{\mathbf{u}}\|^2 - \frac{nH}{2}\langle\frac{m^2c^4}{\hbar^2}\tilde{\mathbf{u}} + \lambda c^2|\tilde{\mathbf{u}}|^{q-1}\tilde{\mathbf{u}},\tilde{\mathbf{u}}\rangle$$

$$
\begin{aligned}
&+ nH\langle\frac{m^2c^4}{2\hbar^2}\tilde{\mathbf{u}}^2+\frac{\lambda c^2}{q+1}|\tilde{\mathbf{u}}|^{q+1},1\rangle]\\
=&\frac{1}{c}e^{nHt}[-Hc^2e^{-2Ht}\|\Lambda^{\alpha/4}\tilde{\mathbf{u}}\|^2-\frac{nH}{2}h\sum_{i=1}^{N}(\frac{m^2c^4}{\hbar^2}\tilde{\mathbf{u}}_\mathbf{i}+\lambda c^2|\tilde{\mathbf{u}}_\mathbf{i}|^{q-1}\tilde{\mathbf{u}}_\mathbf{i})(\tilde{\mathbf{u}}_\mathbf{i})\\
&+\frac{nH}{2}h\sum_{i=1}^{N}(\frac{m^2c^4}{\hbar^2}{\tilde{\mathbf{u}}_\mathbf{i}}^2+\frac{2\lambda c^2}{q+1}|\tilde{\mathbf{u}}_\mathbf{i}|^{q+1}\times 1)]\\
=&\frac{1}{c}e^{nHt}[-Hc^2e^{-2Ht}\|\Lambda^{\alpha/4}\tilde{\mathbf{u}}\|^2-\frac{nH}{2}\frac{m^2c^4}{\hbar^2}\|\tilde{\mathbf{u}}\|^2-\frac{nH}{2}\lambda c^2\|\tilde{\mathbf{u}}\|^{q+1}\\
&+\frac{nH}{2}\frac{m^2c^4}{\hbar^2}\|\tilde{\mathbf{u}}\|^2+\frac{nH}{2}\frac{2\lambda c^2}{q+1}\|\tilde{\mathbf{u}}\|^{q+1}]\\
=&\frac{1}{c}e^{nHt}[-Hc^2e^{-2Ht}\|\Lambda^{\alpha/4}\tilde{\mathbf{u}}\|^2-\frac{nH}{2}\frac{\lambda c^2(q-1)}{q+1}\|\tilde{\mathbf{u}}\|^{q+1}],
\end{aligned}
$$

where $c>0$, $q>1$, and $\|\Lambda^{\frac{\alpha}{4}}u\|^2>0$, the term $\frac{\lambda c^2(q-1)}{q+1}\|u\|^{q+1}$ is non-negative. The behaviors of $\mathcal{E}$ for the semi-discrete system is determined by the coefficient H. When $H>0$, we have $\frac{d}{dt}\mathcal{E}_N(t)<0$, indicating that the system is energy dissipation-preserving, i.e., $\mathcal{E}_N(t)<\mathcal{E}_N(0)$ for $t>0$. When $H<0$, $\frac{d}{dt}\mathcal{E}_N(t)>0$, indicating that the system is energy anti-dissipative which means $\mathcal{E}_N(t)>\mathcal{E}_N(0)$ for $t>0$. When $H=0$, $\frac{d}{dt}\mathcal{E}_N(t)=0$, the system is energy conservative, i.e., $\mathcal{E}_N(t)=\mathcal{E}_N(0)$ for $t>0$.

Similarly, in Example 1.2, for $t\in(0,T]$, we have

$$
\mathcal{E}_N(t)=\left[\frac{1}{2}\|\tilde{\mathbf{u}}_t\|^2+\frac{1}{2}\left\|\Lambda\tilde{\mathbf{u}}\right\|^2+\frac{1}{2!}\|\tilde{\mathbf{u}}\|^2-\frac{1}{4!}\|\tilde{\mathbf{u}}\|^4+\frac{1}{6!}\|\tilde{\mathbf{u}}\|^6\right],
$$

and

$$
\frac{d}{dt}\mathcal{E}_N(t)=\langle\tilde{\mathbf{u}}_{tt},\tilde{\mathbf{u}}_t\rangle+\langle\Lambda\tilde{\mathbf{u}},\tilde{\mathbf{u}}_t\rangle+\langle\tilde{\mathbf{u}},\tilde{\mathbf{u}}_t\rangle-\frac{1}{3}\langle\tilde{\mathbf{u}}^3,\tilde{\mathbf{u}}_t\rangle+\frac{1}{5}\langle\tilde{\mathbf{u}}^5,\tilde{\mathbf{u}}_t\rangle.
$$

Computing the discrete inner product of (2.8) with u_t, we obtain

$$
\langle\tilde{\mathbf{u}}_{tt},\tilde{\mathbf{u}}_t\rangle=-\left[\langle\Lambda\tilde{\mathbf{u}},\tilde{\mathbf{u}}_t\rangle+\langle\tilde{\mathbf{u}}_t,\tilde{\mathbf{u}}_t\rangle+\langle\tilde{\mathbf{u}},\tilde{\mathbf{u}}_t\rangle-\frac{1}{3}\langle\tilde{\mathbf{u}}^3,\tilde{\mathbf{u}}_t\rangle+\frac{1}{5}\langle\tilde{\mathbf{u}}^5,\tilde{\mathbf{u}}_t\rangle\right].
$$

Substituting the computed formula into the above equation, we get

$$
\frac{d}{dt}\mathcal{E}_N(t)=-\|\tilde{\mathbf{u}}_t\|^2<0.
$$

So the energy of the semi-discrete system in Example 1.2 is energy dissipative.

2.3. Temporal discretization

In this subsection, the ERKN method is employed in the temporal discretization and the convergence and stability are investigated.

2.3.1. Extended Runge-Kutta-Nyström-type method for temporal discretization

We now perform a temporal discretization on the spatially semi-discretized system (2.9) that was obtained in the previous section.

Firstly, we introduce the ERKN method, which can effectively solve the following general second-order system

$$\begin{cases} \tilde{\mathbf{u}}_{tt} + Q\tilde{\mathbf{u}} = f(\tilde{\mathbf{u}}, \tilde{\mathbf{u}}_t), \quad t \in (t_0, T], \\ \tilde{\mathbf{u}}(t_0) = \tilde{\mathbf{u}}_0, \quad \tilde{\mathbf{u}}'(t_0) = \tilde{\mathbf{u}}'_0, \end{cases} \tag{2.18}$$

where Q is a diagonal matrix with nonnegative entries. Suggesting $\tau = T/M$ as the temporal step size. To solve the second-order initial value problems (2.18), we use the fourth-order ERKN method proposed by You et al. [26] which is derived from the variation-of-constants formula

$$\begin{aligned} \tilde{\mathbf{u}}(t+\beta\tau) &= \phi_0(\beta^2 V)\tilde{\mathbf{u}}(t) + \beta\phi_1(\beta^2 V)\tau\tilde{\mathbf{u}}'(t) \\ &\quad + \tau^2 \int_0^\beta (\beta - z)\phi_1((\beta - z)^2 V) f(\tilde{\mathbf{u}}(t + z\tau), \tilde{\mathbf{u}}_t(t + z\tau))dz, \\ \tilde{\mathbf{u}}'(t+\beta\tau) &= -\beta\tau Q\phi_1(\beta^2 V)\tilde{\mathbf{u}}(t) + \phi_0(\beta^2 V)\tilde{\mathbf{u}}'(t) \\ &\quad + \tau \int_0^\beta \phi_0((\beta - z)^2 V) f(\tilde{\mathbf{u}}(t + z\tau), \tilde{\mathbf{u}}_t(t + z\tau))\mathrm{d}z, \end{aligned}$$

where $V = \tau^2 Q$, and the matrix-valued ϕ-function is defined by

$$\phi_l(Q) := \sum_{k=0}^{\infty} \frac{(-1)^k Q^k}{(2k+l)!}, \quad l = 0, 1, \ldots.$$

An s-stage ERKN integrator for the numerical integration of the system (2.18) is defined as

$$\begin{aligned} \tilde{\mathbf{U}}_k &= \phi_0\left(c_k^2 V\right)\tilde{\mathbf{u}}_n + c_k\phi_1\left(c_k^2 V\right)\tau\tilde{\mathbf{u}}'_n + \tau^2 \sum_{l=1}^{s} \bar{a}_{kl}(V) f\left(\tilde{\mathbf{U}}_l, \tilde{\mathbf{U}}'_l\right), k = 1, \ldots, s, \\ \tilde{\mathbf{U}}'_k &= -c_i\tau Q\phi_1\left(c_k^2 V\right)\tilde{\mathbf{u}}_n + \phi_0\left(c_k^2 V\right)\tilde{\mathbf{u}}'_n + \tau \sum_{l=1}^{s} a_{kl}(V) f\left(\tilde{\mathbf{U}}_l, \tilde{\mathbf{U}}'_l\right), k = 1, \ldots, s, \\ \tilde{\mathbf{u}}_{n+1} &= \phi_0(V)\tilde{\mathbf{u}}_n + \phi_1(V)\tau\tilde{\mathbf{u}}'_n + \tau^2 \sum_{k=1}^{s} \bar{b}_k(V) f\left(\tilde{\mathbf{U}}_k, \tilde{\mathbf{U}}'_k\right), \\ \tilde{\mathbf{u}}'_{n+1} &= -\tau Q\phi_1(V)\tilde{\mathbf{u}}_n + \phi_0(V)\tilde{\mathbf{u}}'_n + \tau \sum_{k=1}^{s} b_k(V) f\left(\tilde{\mathbf{U}}_k, \tilde{\mathbf{U}}'_k\right), \end{aligned} \tag{2.19}$$

in which the coefficients c_k, $\bar{a}_{kl}$ are matrix-valued functions of V, and coefficient of (2.19) can be expressed as the following Butcher tableau

$$\begin{array}{c|cc} c & A & \bar{A} \\ \hline & b^T(V) & \bar{b}^T(V) \end{array} = \begin{array}{c|cccc|cccc} 0 & 0 & 0 & 0 & 0 & 0 & 0 & 0 & 0 \\ c_2 & a_{21}(V) & 0 & 0 & 0 & 0 & 0 & 0 & 0 \\ c_3 & a_{31}(V) & a_{32}(V) & 0 & 0 & \bar{a}_{31}(V) & 0 & 0 & 0 \\ c_4 & a_{41}(V) & a_{42}(V) & a_{43}(V) & 0 & \bar{a}_{41}(V) & \bar{a}_{42}(V) & 0 & 0 \\ \hline & b_1(V) & b_2(V) & b_3(V) & b_4(V) & \bar{b}_1(V) & \bar{b}_2(V) & \bar{b}_3(V) & \bar{b}_4(V) \end{array}.$$

To better meet the applicable conditions of the ERKN method, we present an equivalent system of the original equation (2.9), let $f(\tilde{\mathbf{u}}, \tilde{\mathbf{u}}_t) = -[\kappa\tilde{\mathbf{u}}_t + \widetilde{G'(\mathbf{u})}]$ and $Q = J(t)\Lambda^{\frac{\alpha}{2}}$, we can rewrite the system into second-order initial value problems of the form (2.18). Then we can immediately solve the problem through above temporal method.

We now define the fully discrete energy of the proposed scheme to distinguish it from the semi-discrete energy. Let

$$E_n(t) = e^{\kappa t}\left[\frac{1}{2}u_n'^T u_n' + \frac{\kappa}{2}\langle u_n', u_n\rangle_x + \frac{J(t)}{2}u_n^T\Lambda^{\alpha/2}u_n + \langle G(u_n), 1\rangle_x\right]. \tag{2.20}$$

This expression serves as a natural numerical analog of the semi-discrete energy given in (2.11).

2.3.2. Stability and convergence analysis

To analyze the linear stability of the ERKN method, we first note that Q is a symmetric positive definite diagonal matrix, so we can set $Q = q^2 I$ with $q > 0$. In many studies, the linear test model $u_{tt} + q^2 u + \eta u = 0$ is used to study stability for systems of the form $u_{tt} + q^2 u + f(u) = 0$. To capture the essential features of our semi-discrete system (2.18), we consider the linear test model

$$\tilde{\mathbf{u}}_{tt} + q^2\tilde{\mathbf{u}} + \eta\tilde{\mathbf{u}}_t = 0, \tag{2.21}$$

where $q > 0$, $\eta > 0$. Applying the ERKN method to this model leads to a recurrence relation. The following theorem states the linear stability criterion for the ERKN method.

Theorem 2.2 (Stability condition of ERKN methods)**.** *Under the linear test model* (2.21)*, the ERKN method* (2.19) *yields the following iteration coefficient matrix*

$$M(\nu,\sigma) = \begin{pmatrix} \phi_0 + \nu^2 S\big(c\phi_1(c^2\nu^2)\big) & \phi_1 - S\phi_0(c^2\nu^2) \\ -\nu^2\phi_1 + \nu^2 S\big(c\phi_1(c^2\nu^2)\big) & \phi_0 - S\phi_0(c^2\nu^2) \end{pmatrix},$$

where $\nu = \tau q$, $\sigma = \tau\eta$, $\phi_0 = \phi_0(\nu^2)$, $\phi_1 = \phi_1(\nu^2)$, $S = \sigma\bar{b}^T(I + \sigma A)^{-1}$. *The method satisfies*

$$\begin{pmatrix} \tilde{\mathbf{u}}_{n+1} \\ \tau\tilde{\mathbf{u}}_{n+1}' \end{pmatrix} = M(\nu,\sigma)\begin{pmatrix} \tilde{\mathbf{u}}_n \\ \tau\tilde{\mathbf{u}}_n' \end{pmatrix}.$$

The stability of ERKN method is determined by the spectral radius $\rho(\cdot)$ *of M. Stability is achieved when* $\rho(M) \le 1$*; in contrast, if* $\rho(M) > 1$*, the method becomes unstable.*

Proof. We utilize the ERKN method (2.19) to solve the linear test model (2.21), and obtain the scheme

$$\tilde{\mathbf{U}}_k = \phi_0(c_k^2 V)\tilde{\mathbf{u}}_n + c_k\phi_1(c_k^2 V)\tau\tilde{\mathbf{u}}_n + \tau^2\sum_{l=1}^{s}\bar{a}_{kl}(V)\eta\tilde{\mathbf{U}}_k',\ k = 1,\dots,s,$$

$$\tilde{\mathbf{U}}_k' = -c_k\tau Q\phi_1(c_k^2 V)\tilde{\mathbf{u}}_n + \phi_0(c_k^2 V)\tilde{\mathbf{u}}_n' + \tau\sum_{l=1}^{s}a_{kl}(V)\eta\tilde{\mathbf{U}}_k',\ k = 1,\dots,s,$$

$$\tilde{\mathbf{u}}_{n+1} = \phi_0(V)\tilde{\mathbf{u}}_n + \phi_1(V)\tau\tilde{\mathbf{u}}_n' + \tau^2\sum_{k=1}^{s}\bar{b}_k(V)\eta\tilde{\mathbf{U}}_k',$$

$$\tilde{\mathbf{u}}'_{n+1} = -\tau Q\phi_1(V)\tilde{\mathbf{u}}_n + \phi_0(V)\tilde{\mathbf{u}}'_n + \tau\sum_{k=1}^{s} b_k(V)\eta\tilde{\mathbf{U}}'_k,$$

where $V = \tau^2 Q$.

Then, by letting $\nu = \tau q$, $\sigma = \tau\eta$, since $V = \tau^2 Q = (\tau q)^2 I = \nu^2 I$, we have the following compact iterative form of (2.21) as

$$\begin{aligned}
&\tilde{\mathbf{U}} = \phi_0(c^2\nu^2)\otimes\tilde{\mathbf{u}}_n + c\phi_1(c^2\nu^2)\otimes\tau\tilde{\mathbf{u}}'_n - \sigma\bar{A}\tau\tilde{\mathbf{U}}',\\
&\tau\tilde{\mathbf{U}}' = -c\phi_1(c^2\nu^2)\nu^2\otimes\tilde{\mathbf{u}}_n + \phi_0(c^2\nu^2)\otimes\tau\tilde{\mathbf{u}}'_n - A\sigma\tau\tilde{\mathbf{U}}',\\
&\tilde{\mathbf{u}}_{n+1} = \phi_0\tilde{\mathbf{u}}_n + \phi_1\tau\tilde{\mathbf{u}}'_n - \sigma\bar{b}^T\tau\tilde{\mathbf{U}}',\\
&\tau\tilde{\mathbf{u}}'_{n+1} = \phi_0\tau\tilde{\mathbf{u}}'_n - \nu^2\phi_1\tilde{\mathbf{u}}_n - \sigma b^T\tau\tilde{\mathbf{U}}',
\end{aligned} \tag{2.22}$$

where $\phi_0 = \phi_0(\nu^2), \phi_1 = \phi_1(\nu^2)$ and $\phi_k(c^2\nu^2) = (\phi_k(c_1^2\nu^2),\cdots,\phi_k(c_s^2\nu^2))^{\mathrm{T}}, k = 0, 1$. Define operator $\otimes$ as the Kronecker product.

Utilizing the matrix expression in Butcher tableau of the coefficients for ERKN, the expression of $\tau\mathbf{U}'$ in (2.22) has

$$\tau\tilde{\mathbf{U}}' = (I+\sigma A)^{-1}\left(-c\phi_1(c^2\nu^2)\nu^2\otimes\tilde{\mathbf{u}}_n + \phi_0(c^2\nu^2)\otimes\tau\tilde{\mathbf{u}}'_n\right).$$

Substituting the second equation of (2.22) into the last two equations and letting $S = \sigma\bar{b}^T(I+\sigma A)^{-1}$, we obtain the matrix form

$$\begin{pmatrix}\tilde{\mathbf{u}}_{n+1}\\ \tau\tilde{\mathbf{u}}'_{n+1}\end{pmatrix} = \begin{pmatrix}\phi_0 + \nu^2 S(c\phi_1(c^2\nu^2)) & \phi_1 - S\phi_0(c^2\nu^2)\\ -\nu^2\phi_1 + \nu^2 S(c\phi_1(c^2\nu^2)) & \phi_0 - S\phi_0(c^2\nu^2)\end{pmatrix}\begin{pmatrix}\tilde{\mathbf{u}}_n\\ \tau\tilde{\mathbf{u}}'_n\end{pmatrix}.$$

Then, we obtain the iteration coefficient matrix of equation (2.22) as

$$M(\nu,\sigma) = \begin{pmatrix}\phi_0 + \nu^2 S(c\phi_1(c^2\nu^2)) & \phi_1 - S\phi_0(c^2\nu^2)\\ -\nu^2\phi_1 + \nu^2 S(c\phi_1(c^2\nu^2)) & \phi_0 - S\phi_0(c^2\nu^2)\end{pmatrix}.$$

□

Additionally, the plot of the stability region for the equation (2.21) is shown in [15].

For the convergence analysis of ERKN methods, You et al. [26] derived the following necessary and sufficient order conditions.

We first recall the definition of EN-trees (Extended Nyström trees): Rooted trees whose vertices are either meager(representing dependence on y) or fat(representing dependence on y'), used to encode the elementary differentials of $f(y, y')$. For each EN-tree t, let $\rho(t)$ denote its order (number of vertices), $\tilde{\gamma}(t)$ its signed density, and $\Phi_i(t)$ the elementary weight for the i-th stage (defined recursively in [26]).

Theorem 2.3 (Order conditions for ERKN methods)**.** *An ERKN method defined by* (2.19) *has order p if and only if*

$$\begin{aligned}
&\sum_{i=1}^{s}\bar{b}_i(V)\,\Phi_i(t) = \frac{\rho(t)!}{\tilde{\gamma}(t)}\,\phi_{\rho(t)+1}(V) + \mathcal{O}(\tau^{p-\rho(t)}), \quad \forall t\in ENT,\ \rho(t)\le p-1,\\
&\sum_{i=1}^{s}b_i(V)\,\Phi_i(t) = \frac{\rho(t)!}{\tilde{\gamma}(t)}\,\phi_{\rho(t)}(V) + \mathcal{O}(\tau^{p-\rho(t)+1}), \quad \forall t\in ENT,\ \rho(t)\le p,
\end{aligned}$$

where $V = \tau^2\Omega$, and ENT denotes the set of all EN-trees.

In this paper, we use a fourth order ERKN method named as ERKN4, to further study, we give the particular Taylor expansions of the coefficients of ERKN4 method.

$$
\begin{aligned}
&c_2=\frac{1}{5},\ c_3=\frac{2}{3},\ c_4=1,\ a_{31}(V)=-\frac{17}{27}I,\ a_{42}(V)=-\frac{22}{7}I,\ a_{41}(V)=\frac{13}{5}I,\\
&a_{21}(V)=\frac{1}{5}I-\frac{1}{375}V+\frac{1}{125000}V^2-\frac{1}{98437500}V^3+\frac{11}{14175000000}V^4+\cdots,\\
&a_{32}(V)=\frac{35}{27}I-\frac{59}{810}V+\frac{17}{9720}V^2-\frac{223891}{34445250000}V^3+\frac{11747443}{1116026100000000}V^4+\cdots,\\
&a_{43}(V)=\frac{54}{35}I-\frac{4}{75}V+\frac{89}{135000}V^2-\frac{64891}{318937500}V^3-\frac{143450723}{3444525000000}V^4+\cdots,\\
&b_1(V)=\frac{1}{24}I-\frac{1}{40}V+\frac{19}{8064}V^2-\frac{1}{12960}V^3+\cdots,\\
&b_2(V)=\frac{125}{336}I-\frac{25}{224}V+\frac{625}{112896}V^2-\frac{5}{41472}V^3+\cdots,\\
&b_3(V)=\frac{27}{56}I-\frac{9}{280}V+\frac{3}{6272}V^2+\cdots,\\
&b_4(V)=\frac{5}{48}I+\frac{1}{480}V-\frac{1}{26880}V^2-\frac{1}{1451520}V^3+\cdots,\\
&\bar{b}_1(V)=\frac{1}{24}I+\frac{29}{5040}V-\frac{491}{4233600}V^2+\cdots,\\
&\bar{b}_2(V)=\frac{25}{84}I-\frac{775}{14112}V+\frac{2293}{1185408}V^2+\cdots,\\
&\bar{b}_3(V)=\frac{9}{56}I+\frac{57}{3920}V-\frac{8071219}{388962000000}V^2+\cdots,\\
&\bar{b}_4(V)=-\frac{71}{10080}V+\frac{1243}{4233600}V^2+\cdots,\\
&\bar{a}_{31}(V)=a_{32}a_{21},\quad \bar{a}_{41}(V)=a_{42}(V)a_{21}(V)+a_{43}(V)a_{31}(V),\quad \bar{a}_{42}(V)=a_{43}(V)a_{32}(V).
\end{aligned}
$$

2.4. Extension to multi-dimensional problem

For the matrix representation of the Riesz space-fractional derivative with homogeneous Dirichlet boundary conditions, assuming $U^{(2)}=\{u_{i,j}\}_{(N-1)\times(N-1)}$, the matrix representation of the two-dimensional Riesz space-fractional derivative can be expressed as

$$(-\Delta)^{\alpha/2}U^{(2)}=L_x^{\alpha/2}U^{(2)}+U^{(2)}(L_y^{\alpha/2})^T,$$

where $L_x=A^{-1}B$, $L_y=A^{-1}B$ with the matrices A, B are given by (2.5).

Defining operator $\textcircled{x}$ and $\textcircled{y}$ as $L_x\textcircled{x}U^{(2)}=L_xU^{(2)}$, $L_y\textcircled{y}U^{(2)}=U^{(2)}L_y^T$, where

$$(L_x\textcircled{x}U^{(2)})_{k,l}=\sum_{n=1}^{N}(L_x)_{k,n}u_{n,l},\quad \left(L_y\textcircled{y}U^{(2)}\right)_{i,j}=\sum_{n=1}^{N}(L_y)_{i,n}u_{j,n}.$$

Define the operator $\odot$ for the element-by-element multiplication of two arrays of the same size as

$$(A\odot B)_{i,j}=(B\odot A)_{i,j}=A_{i,j}B_{i,j}.$$

Then, we can obtain the following representation

$$(-\Delta)^{\alpha/2}u(x,y,t)=P_y^{-1}\textcircled{y}P_x^{-1}\textcircled{x}\left(\Lambda^{\alpha/2}\odot\left(P_y\textcircled{y}P_x\textcircled{x}U^{(2)}\right)\right),\tag{2.23}$$

where

$$(\Lambda^{\alpha/2})_{i,j} = \left(\left(\frac{4\sin^2(\frac{i\pi}{2N})}{h^2(1-\frac{1}{3}\sin^2(\frac{i\pi}{2N}))} \right)^{\alpha/2} + \left(\frac{4\sin^2(\frac{j\pi}{2N})}{h^2(1-\frac{1}{3}\sin^2(\frac{j\pi}{2N}))} \right)^{\alpha/2} \right),$$

where $i, j = 1, \cdots, N-1$. The orthogonal matrices P_x and P_y are given in (2.7).

Substituting (2.23) into system (2.9) yields the spatial discretization of two-dimensional nonlinear generalized damped FKGE as

$$\widetilde{U_{tt}^{(2)}} + J(t)\Lambda^{\alpha/2} \odot \widetilde{U^{(2)}} + \kappa \widetilde{U^{(2)}}_t + \widetilde{G'(U^{(2)})} = 0, \tag{2.24}$$

where $\widetilde{U^{(2)}} = P_y \textcircled{y} P_x \textcircled{x} U^{(2)}$, $\widetilde{U_{tt}^{(2)}} = P_y \textcircled{y} P_x \textcircled{x} U_{tt}^{(2)}$, $\widetilde{U_t^{(2)}} = P_y \textcircled{y} P_x \textcircled{x} U_t^{(2)}$ and $\widetilde{G'(U^{(2)})} = P_y \textcircled{y} P_x \textcircled{x} G'(U^{(2)})$.

Following the same procedure and setting $U^{(2)} = \{u_{i,j}\}_{(N+1)\times(N+1)}$, we obtain the FKGE with homogeneous Neumann boundary conditions where

$$(\Lambda^{\alpha/2})_{i,j} = \left(\left(\frac{4\sin^2(\frac{i\pi}{2N})}{h^2(1-\frac{1}{3}\sin^2(\frac{i\pi}{2N}))} \right)^{\alpha/2} + \left(\frac{4\sin^2(\frac{j\pi}{2N})}{h^2(1-\frac{1}{3}\sin^2(\frac{j\pi}{2N}))} \right)^{\alpha/2} \right),$$

where $i, j = 0, \cdots, N$, and $\widetilde{U^{(2)}} = P_y \textcircled{y} P_x \textcircled{x} U^{(2)}$, $\widetilde{G'(U^{(2)})} = P_y \textcircled{y} P_x \textcircled{x} G'(U^{(2)})$, the orthogonal matrices P_x and P_y are given in (2.10).

The multi-dimensional temporal methods are similar to the temporal schemes given in Section 2.3, we use the two-dimensional ERKN method for the two-dimensional semi-discrete system (2.24).

In addition, we observe that in multi-dimensional cases, the nonlinear systems will result in large-scale matrices, which increases the difficulty of matrix function computations in the temporal direction and demands substantial storage space. According to [20], the Krylov subspace methods were adopted to deal with the large-scale matrix. Moreover, to reduce the computational complexity of numerical methods, we can further use an adaptive Antoulas–Anderson method [6] and a sketched Full Orthogonalization Method [7].

3. Numerical experiments

In this part, we will verify the effectiveness and accuracy of the present numerical method through various numerical examples. First, we will verify the convergence order and numerical accuracy of the method. Then, we will observe the influence of different parameters on the numerical solution.

To verify the accuracy and efficiency of the proposed schemes, we compute the numerical errors via the formula

$$\|u - u_{h,\tau}\|_\infty = \max |u(\boldsymbol{x}, t) - u_n^M|,$$

where $u(\boldsymbol{x}, t)$ and u_n^M are the n-th exact and numerical solutions at time t, respectively. Additionally, the order of convergence in space is computed as

$$\text{Order} = \log_2 \left(\frac{E_{h,\tau}}{E_{h/2,\tau/2}} \right),$$

where $E_{h,\tau} = \|u(\boldsymbol{x}, t) - u_{h,\tau}\|_\infty$ and $E_{h/2,\tau/2} = \|u(\boldsymbol{x}, t) - u_{h/2,\tau/2}\|_\infty$ with spatial step size h and temporal step size $\boldsymbol{\tau}$.

3.1. One-dimensional problems

Consider the following FKGE subject to the homogeneous boundary conditions

$$u_{tt} + (-\Delta)^{\alpha/2} u + \kappa u_t + G'(u) = 0, \quad \boldsymbol{x} \in \Omega, \quad t > 0, \quad 1 < \alpha \leq 2, \tag{3.1}$$

where $G(u) = 1 - \cos(u)$, $\kappa \geq 0$, when $\alpha = 2$, and the equation has following exact solution

$$u(x,t) = 4 \arctan\left(\frac{\sqrt{1-\omega^2}\cos(\omega t)}{\omega \cosh(\sqrt{1-\omega^2}x)} \right), \forall (x,t) \in \Omega \times (0,T].$$

In the first test, we consider the equation (3.1) in domain $\Omega = (-40, 40)$ and $t \in (0, 20]$, and let $\omega = 0.9$. In Figure 1, the simulated solution and the corresponding absolute errors demonstrate excellent agreement between the proposed numerical method and the exact solution for $\alpha = 2$. Figure 1 (c) shows that the breather-like solution is periodic in time, which is in

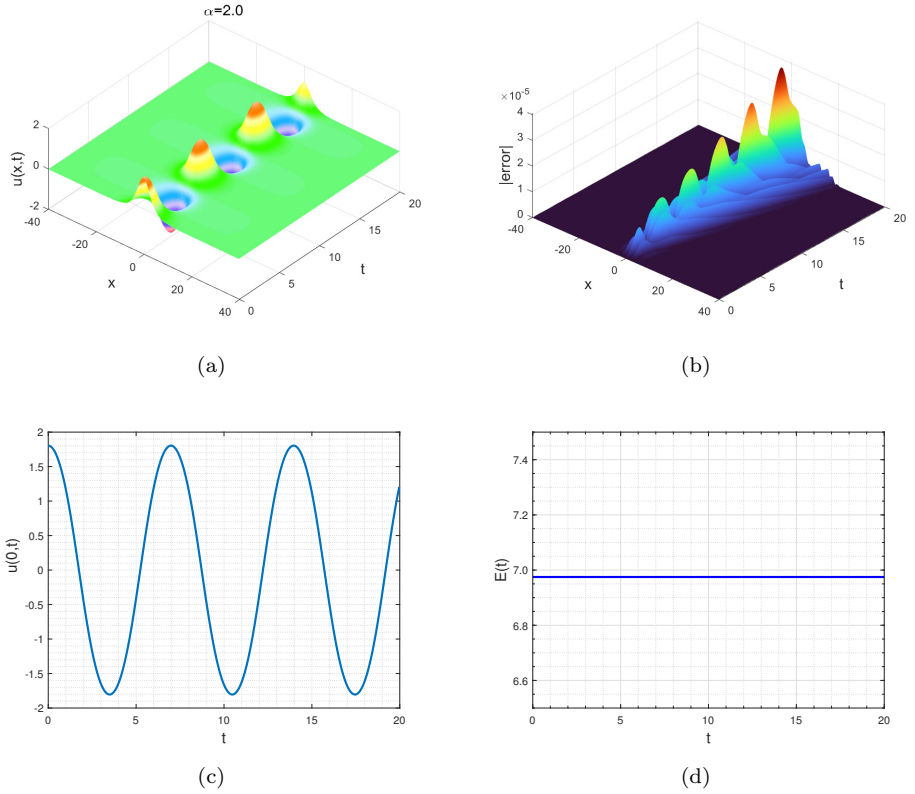

Figure 1. Snapshots corresponding to (a) the numerical solution, (b) the absolute error of the numerical solution, (c) the time evolution of the $u(0,t)$, and (d) the time evolution of the approximate total energy with $\alpha = 2$ and $N = 256$ and $M = 1000$ for equation (3.1).

excellent agreement with the theory. The total energy behavior of the solution is displayed in Figure 1 (d), which confirms that the system's energy is conservative.

In order to study the convergence of the proposed method, we test the efficiency and convergence order of the fractional difference scheme with MTT by comparing the results with different spatial and temporal steps and fractional orders. So we fix $M = 1000$ in Table 1 and

$N = 250$ in Table 2, computing the results using the MTT for different values of α, N and M. Tables 1 and 2 present the maximum errors and convergence orders of the proposed numerical method. From Table 1, we observe that the proposed numerical method achieves fourth order

Table 1. Comparison of accuracy for equation (3.1) with $M = 1000$.

N	$\alpha = \mathbf{1.1}$		$\alpha = \mathbf{1.5}$		$\alpha = \mathbf{1.9}$		$\alpha = \mathbf{2.0}$	
	Error	Order	Error	Order	Error	Order	Error	Order
20	3.6846e-03	–	1.0114e-03	–	8.2395e-05	–	8.0079e-05	–
40	1.9083e-04	4.27	6.2467e-05	4.02	4.9901e-06	4.05	5.3969e-06	3.89
80	4.4433e-06	5.42	1.5845e-06	5.30	1.3789e-07	5.18	3.8947e-07	3.79
160	2.5755e-07	4.11	9.7189e-08	4.03	1.1240e-08	3.62	2.0378e-08	4.26

Table 2. Comparison of accuracy for equation (3.1) with $N = 250$.

M	$\alpha = \mathbf{1.1}$		$\alpha = \mathbf{1.5}$		$\alpha = \mathbf{1.9}$		$\alpha = \mathbf{2.0}$	
	Error	Order	Error	Order	Error	Order	Error	Order
100	7.3410e-08	–	1.7555e-08	–	1.3843e-09	–	5.6055e-12	–
200	7.0242e-09	3.39	1.7050e-09	3.36	1.3441e-10	3.36	2.9451e-13	4.25
400	5.8972e-10	3.57	1.4425e-10	3.56	1.1366e-11	3.56	1.9387e-14	3.93
800	4.6076e-11	3.68	1.1322e-11	3.69	8.8286e-13	3.69	1.3306e-15	3.86
1600	3.2521e-12	3.82	8.0809e-13	3.81	4.9387e-14	4.16	5.3717e-17	4.63

accuracy in space. Table 2 also confirms that the temporal method achieves the theoretical convergence. Furthermore, it attains the high-order accuracy predicted by theoretical analysis, validating both the efficiency and high precision of our proposed methodology.

Figure 2 displays the numerical solutions and total energy dynamics for fractional orders $\alpha = 1.1$, 1.5, and 1.9, with fixed spatial resolution $N = 256$ and temporal steps $M = 700$. The total energy is a constant function of time. This conservation property aligns with the theoretical analysis in Section 2, demonstrating that our scheme exactly preserves the discrete energy conservation laws. Our approach achieves good performance and high efficiency.

Next, we consider the Riesz space fractional Klein-Gordon equation (1.1) in the de Sitter space. We let $h(t) = e^{-2Ht}$ and $G(u) = -\frac{1}{20}u^2 + \frac{1}{2}|u|^4$. The initial conditions for the Klein-Gordon problem are given by $u(x,0) = \varphi_{0.5,0.3}(x)$ and $u_t(x,0) = 0$

$$\varphi_{b_1,b_2}(x) = \begin{cases} e^{\frac{1}{b_2^2} - \frac{1}{b_2^2 - (x-b_1)^2}}, & \text{if } |x-b_1| < b_2, \\ 0, & \text{if } b_2 \le |x-b_1|. \end{cases}$$

We conduct numerical simulations by varying the Hubble constant H to investigate its influence on the system's dynamics. Figures 3 (a-e) show the dynamic behavior of the numerical solution in an expanding spacetime ($H > 0$), while Figure 3 (f) demonstrates the corresponding dissipative property $E(t) < E(0)$ for $t > 0$. Similarly, Figures 4 (a-e) depict the solution in

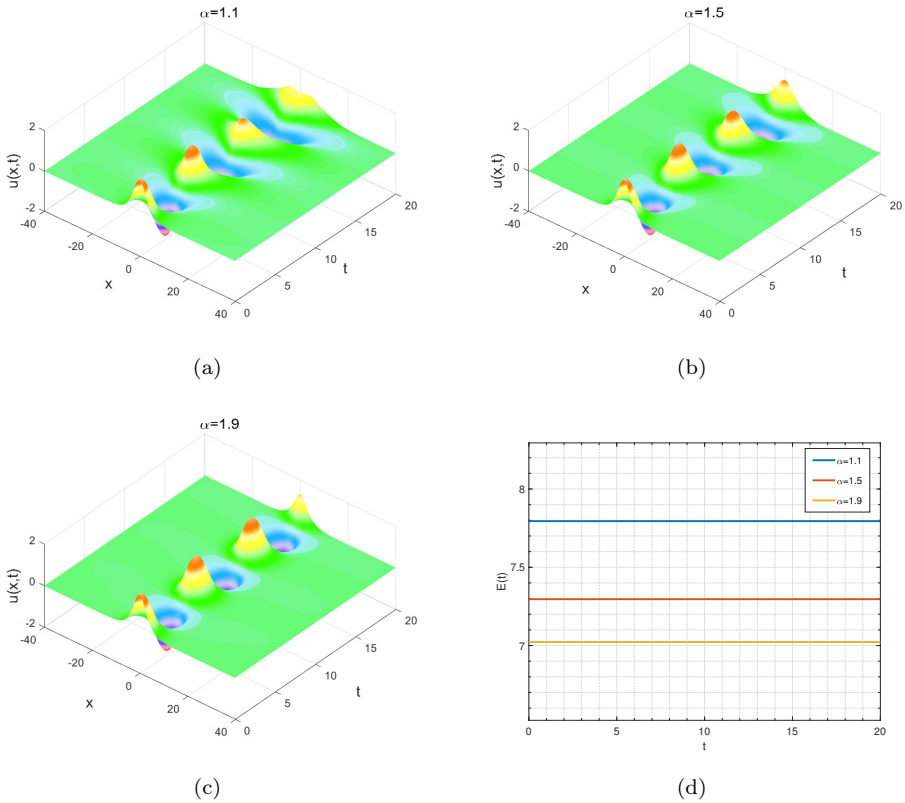

Figure 2. Graphs corresponding to (a) the numerical solution of $\alpha = 1.1$, (b) the numerical solution of $\alpha = 1.5$, (c) the numerical solution of $\alpha = 1.9$, and (d) the time evolution of the approximate total energy with $N = 256$ and $M = 700$ for equation (3.1) with varying α.

a flat spacetime ($H = 0$), and Figure 4 (f) confirms the conservative property $E(t) = E(0)$. Finally, Figures 5 (a-e) and 5 (f) reveal the dynamic behavior and the anti-dissipative property $E(t) > E(0)$ in a contracting spacetime ($H < 0$), respectively. In conclusion, these results demonstrate that E can not be conserved during time evolution when the Hubble constant $H \neq 0$. Furthermore, the behavior of E reflects the dynamical effects induced by spatial contraction and expansion through the Hubble constant H.

3.2. Two-dimensional problem

The method proposed in this paper has been generalized to solve two-dimensional problems in Section 2.4. In this part, we investigate the performance of the present scheme for the Riesz space-fractional generalized damped Klein-Gordon equations in two spatial dimensions by considering the two-dimensional problem (1.1) with $G(u) = \frac{u^4}{4}$, $\kappa = 0$ on domain $(-10, 10) \times (-10, 10) \times (0, T]$, and the initial values are given as

$$\varphi(x, y) = \frac{2}{\cosh\left(\cosh\left(x^2 + y^2\right)\right)}, \quad \mu(x, y) = 0, \quad (x, y) \in (-10, 10) \times (-10, 10).$$

In order to test the energy dissipation law, we define the discrete relative energy error for

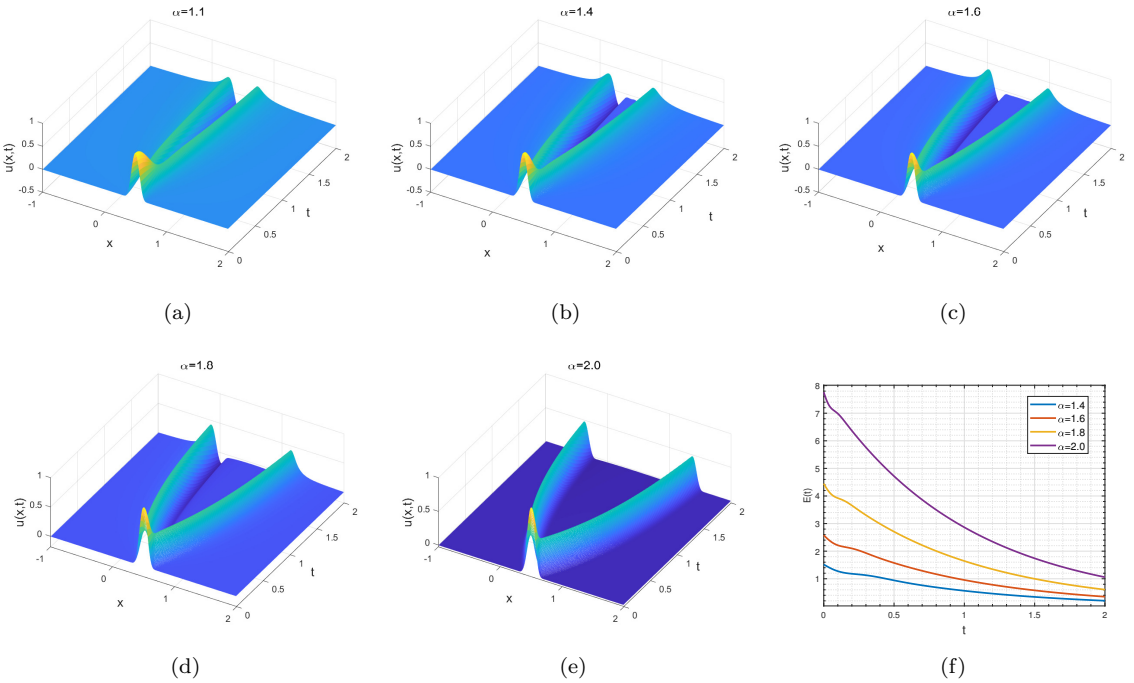

Figure 3. The numerical solution and the energy of FKGE in the de Sitter space at $H = 1$ with $N = 256$ and $M = 400$, for various fractional orders α (the values of α are indicated in the legend).

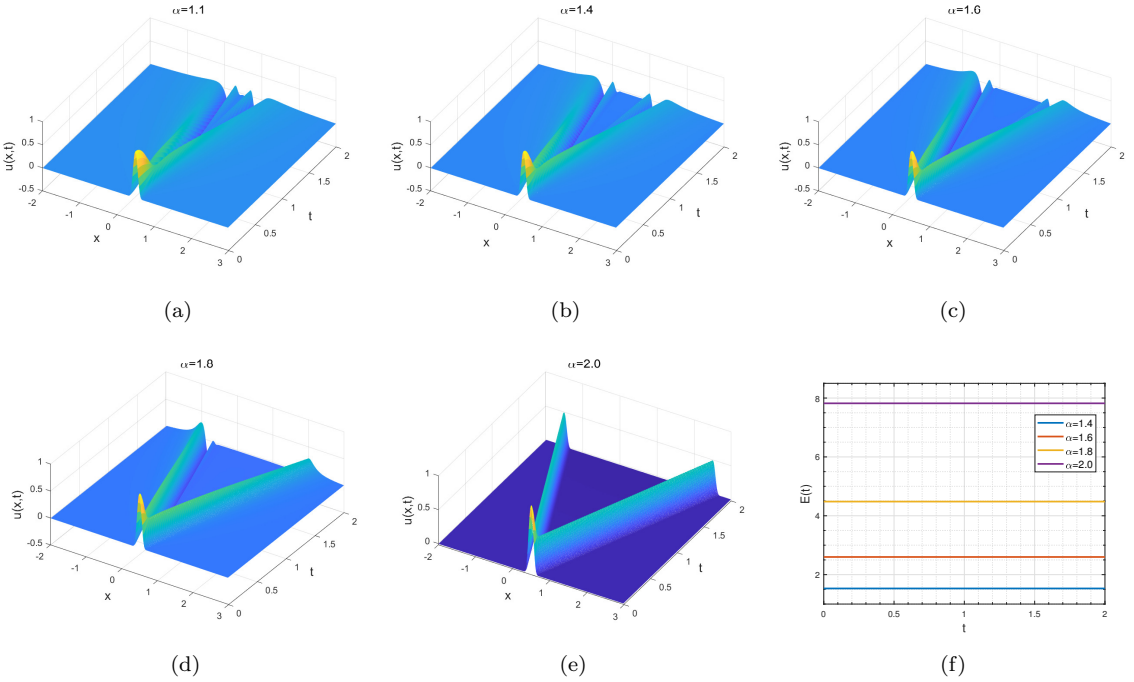

Figure 4. The numerical solution and the energy of FKGE in the de Sitter space at $H = 0$ with $N = 256$, $M = 400$, for various fractional orders α (the values of α are indicated in the legend).

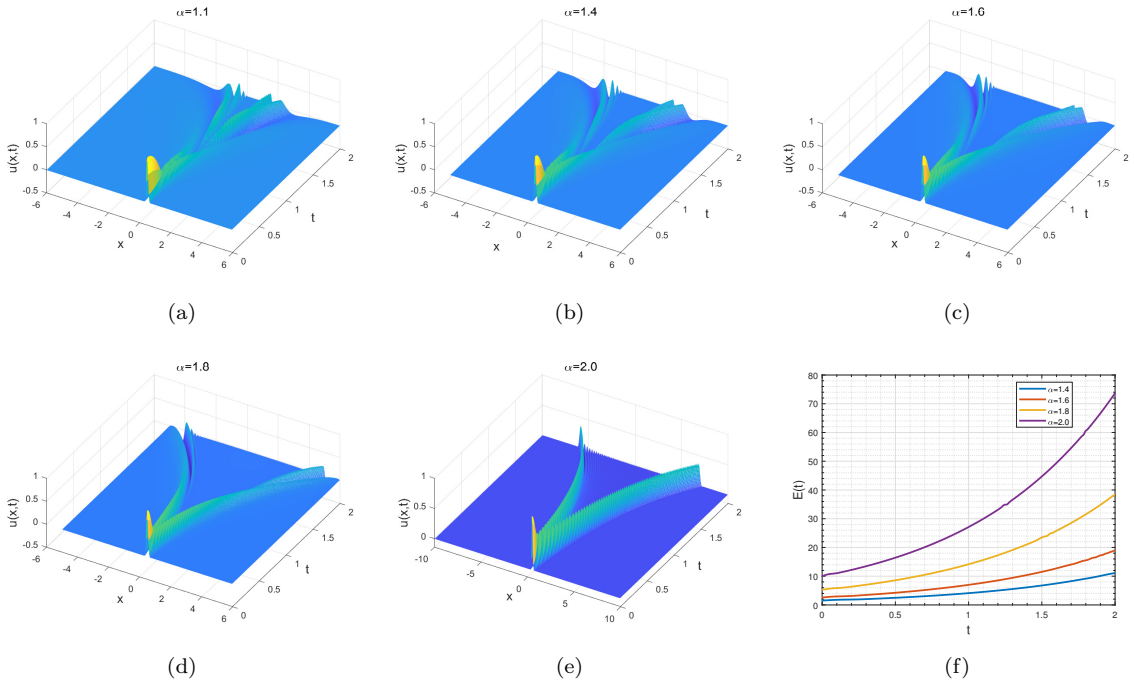

Figure 5. The numerical solution and the energy of FKGE in the de Sitter space at $H = -1$ with $N = 256$, $M = 400$, for various fractional orders α (the values of α are indicated in the legend).

the fully discrete energy in (2.20) as

$$RE_n = |(E_n - E_0)/E_0|, \quad 0 \le n \le N,$$

and the error in discrete dissipation-preserving law is defined as

$$EDL_n = |\delta_t E_n + \kappa \|\delta_t \tilde{\mathbf{u}}_n\|^2|, \quad 0 \le n \le N.$$

Figures 6-8 display numerical solutions under undamped conditions for varying α values. These solutions show excellent agreement with the $\alpha = 2$ case presented in [2]. We observe that at $\alpha = 2$, the soliton reaches the boundary faster than in fractional cases. The plots illustrate the initial soliton profile expanding and propagating throughout the domain until it reaches the boundary.

Figure 9 displays the long time evolution of relative energy errors and the errors in dissipation-preserving law with, which demonstrates the efficiency of our scheme.

4. Conclusions

In this work, we develop a high-precision and easily implementable dissipation-preserving fast numerical scheme for solving the nonlinear generalized damped space-fractional Klein-Gordon equation. The proposed method combines fourth-order ERKN time integration with fourth-order compact finite difference spatial approximation, employing matrix transfer techniques and FFT-based fast computation to enhance computational efficiency. Convergence analysis through numerical experiments and local truncation error calculations demonstrates that the algorithm

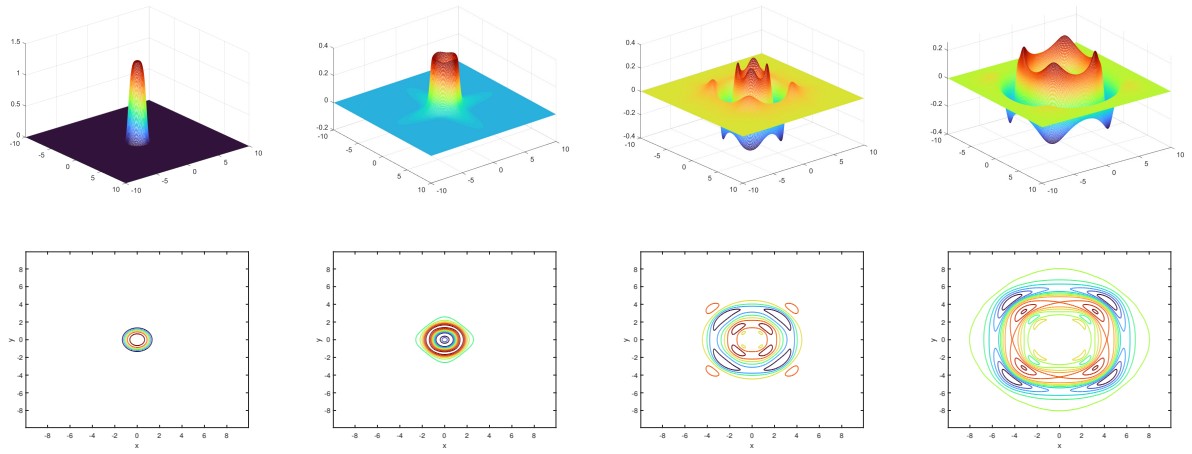

Figure 6. Snapshots of the evolution of the approximate solution for 2D model with $N = 250$, $M = 300$ and $\alpha = 1.5$, at $T = 0$, 1, 5, 8 (Left-Right).

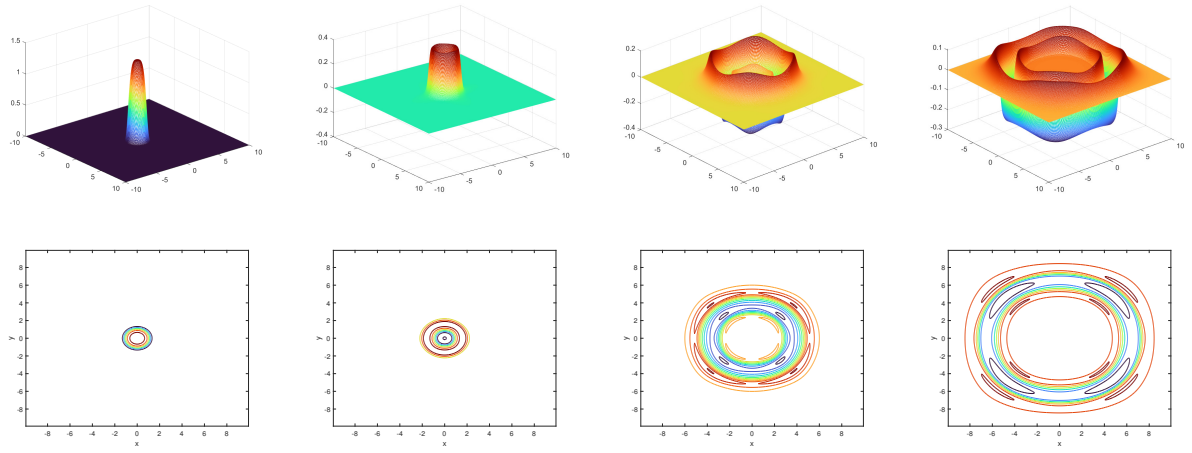

Figure 7. Snapshots of the evolution of the approximate solution for 2D model with $N = 250$, $M = 300$ and $\alpha = 1.8$, at $T = 0$, 1, 5, 8 (Left-Right).

achieves fourth-order accuracy. The approach can be extended to solve the nonlinear generalized damped space-fractional Klein-Gordon equation in two dimensions. Experimental results confirm that this numerical method efficiently and accurately simulates higher-dimensional systems. Numerical experiments under various physical conditions provide comprehensive observations of the energy evolution and confirm the excellent dissipation-preserving properties of the proposed scheme for the nonlinear generalized damped space-fractional Klein-Gordon equation.

Acknowledgements

The authors would like to thank editors and anonymous referees for their valuable comments, which have helped to improve the paper greatly.

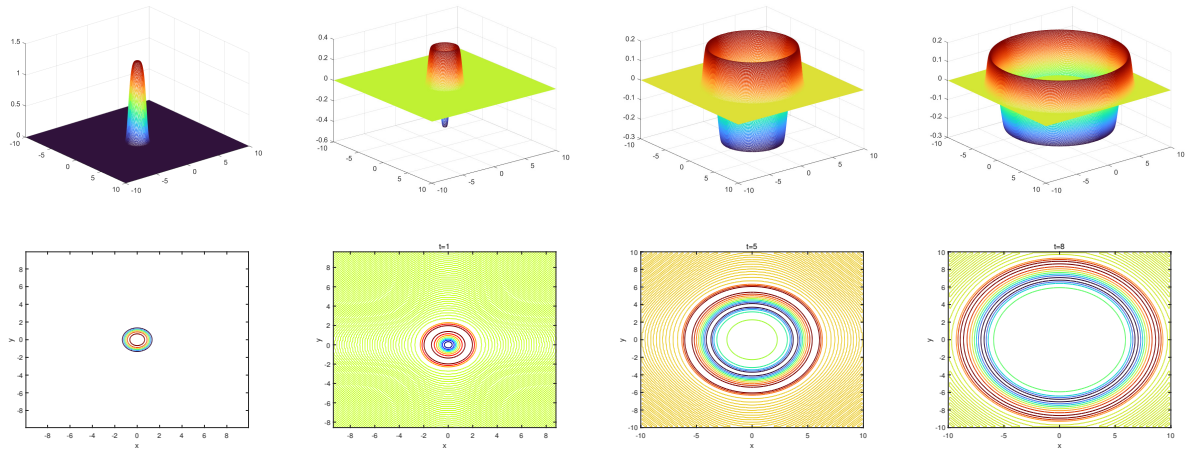

Figure 8. Snapshots of the evolution of the approximate solution for 2D model with $N = 250$, $M = 300$ and $\alpha = 2$, at $T = 0$, 1, 5, 8 (Left-Right).

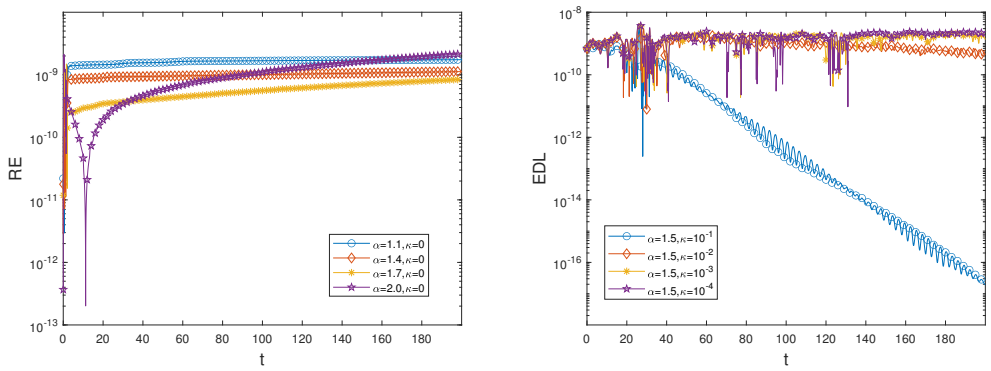

(a) (b)

Figure 9. (a) Temporal progression of the relative energy errors and (b) the dissipation-preserving law under the parameters $h = 1/5$ and $\tau = 1/40$, for various values of α and κ.

References

[1] M. Alkhateeb and A. Matzkin, *Relativistic Bohmian trajectories and Klein-Gordon currents for spin-0 particles*, Found. Phys., 2022, 52(5), 104.

[2] M. A. Darani, *Direct meshless local Petrov–Galerkin method for the two-dimensional Klein–Gordon equation*, Eng. Anal. Bound. Elem., 2017, 74, 1–13.

[3] J. E. Macías-Díaz, *Numerical study of the process of nonlinear supratransmission in Riesz space-fractional sine-Gordon equations*, Commun. Nonlinear Sci. Numer. Simul., 2017, 46, 89–102.

[4] J. E. Macías-Díaz, *A dissipation-preserving scheme to approximate radially symmetric solutions of the Higgs boson equation in the de Sitter space-time*, Commun. Nonlinear Sci. Numer. Simul., 2021, 96, 105698.

[5] H. Ding and Y. Zhang, *New numerical methods for the Riesz space fractional partial differential equations*, Comput. Math. Appl., 2012, 63(7), 1135–1146.

[6] I. V. Gosea and S. Guttel, *Algorithms for the rational approximation of matrix-valued functions*, SIAM J. Sci. Comput., 2021, 43(5), A3033–A3054.

[7] S. Güttel and M. Schweitzer, *Randomized sketching for Krylov approximations of large-scale matrix functions*, SIAM J. Matrix Anal. Appl., 2023, 44(3), 1073–1095.

[8] A. S. Hendy, T. R. Taha, D. Suragan and M. A. Zaky, *An energy-preserving computational approach for the semilinear space fractional damped Klein–Gordon equation with a generalized scalar potential*, Appl. Math. Model., 2022, 108, 512–530.

[9] B. Hou and D. Liang, *Time fourth-order energy-preserving AVF finite difference method for nonlinear space-fractional wave equations*, J. Comput. Appl. Math., 2021, 386, 113227.

[10] Q. Huang, G. Zhang and B. Wu, *Fully-discrete energy-preserving scheme for the space-fractional Klein-Gordon equation via Lagrange multiplier type scalar auxiliary variable approach*, Math. Comput. Simul., 2022, 192, 265–277.

[11] H. Jiang and D. Hu, *Energy dissipation-preserving GSAV-Fourier–Galerkin spectral schemes for space-fractional nonlinear wave equations in multiple dimensions*, Commun. Nonlinear Sci. Numer. Simul., 2024, 128, 107587.

[12] L. Ju, J. Zhang, L. Zhu and Q. Du, *Fast explicit integration factor methods for semilinear parabolic equations*, J. Sci. Comput., 2015, 62(2), 431–455.

[13] M. M. Khader and S. Kumar, *An accurate numerical method for solving the linear fractional Klein–Gordon equation*, Math. Methods Appl. Sci., 2014, 37(18), 2972–2979.

[14] E.-A. Kontou and N. Rothe, *A new approach in classical Klein–Gordon cosmology: 'Small bangs', inflation and dark energy*, Class. Quantum Gravity, 2025, 42(5), 055012.

[15] K. Liu, T. Fu and W. Shi, *Stability analysis for explicit ERKN methods solving general second-order oscillatory systems*, Bull. Malays. Math. Sci. Soc., 2021, 44(6), 4143–4154.

[16] C. Van Loan, *Computational Frameworks for the Fast Fourier Transform*, Society for Industrial and Applied Mathematics, Philadelphia, 1992.

[17] I. Podlubny, *Fractional Differential Equations: An Introduction to Fractional Derivatives, Fractional Differential Equations, to Methods of their Solution and some of their Applications*, Elsevier, Amsterdam, 1998.

[18] A. M. Pombo and I. Saltas, *A Sun-like star orbiting a boson star*, Mon. Not. R. Astron. Soc., 2023, 524(3), 4083–4090.

[19] S. Z. Rida, A. A. M. Arafa, H. S. Hussein, et al., *Residual power series scheme treatments for fractional Klein–Gordon problem arising in soliton theory*, Sci. Rep., 2024, 14(1), 30596.

[20] Y. Saad, *Iterative Methods for Sparse Linear Systems*, Society for Industrial and Applied Mathematics, Philadelphia, 2003.

[21] S. G. Samko, A. A. Kilbas and O. I. Marichev, *Fractional Integrals and Derivatives: Theory and Applications*, Gordon and Breach Science Publishers, London, 1993.

[22] Z. Sun, Y. Liu, B. Yin and H. Li, *Fast structure-preserving difference algorithm for 2D nonlinear space-fractional wave models*, Comput. Math. Appl., 2022, 123, 40–58.

[23] T. Tsuchiya and M. Nakamura, *On the numerical experiments of the Cauchy problem for semi-linear Klein–Gordon equations in the de Sitter spacetime*, J. Comput. Appl. Math., 2019, 361, 396–412.

[24] Z. Wang and S. Vong, *A compact difference scheme for a two dimensional nonlinear fractional Klein–Gordon equation in polar coordinates*, Comput. Math. Appl., 2016, 71(12), 2524–2540.

[25] S. Weinberg, *Gravitation and Cosmology: Principles and Applications of the General Theory of Relativity*, John Wiley & Sons, New York, 1972.

[26] X. You, J. Zhao, H. Yang, et al., *Order conditions for RKN methods solving general second-order oscillatory systems*, Numer. Algorithms, 2014, 66(1), 147–176.

[27] Y. Zhou, J. Xie and Z. Zhang, *Highly efficient difference methods for stochastic space fractional wave equation driven by additive and multiplicative noise*, Appl. Math. Lett., 2021, 116, 106988.

[28] P. Zhuang, F. Liu, V. Anh and I. Turner, *Numerical methods for the variable-order fractional advection-diffusion equation with a nonlinear source term*, SIAM J. Numer. Anal., 2009, 47(3), 1760–1781.

Received December 2025; Accepted July 2026; Available online August 2026.